Crystal structure of quinohemoprotein alcohol dehydrogenase from Comamonas testosteroni - Structural basis for substrate oxidation and electron transfer

Oubrie, A; Rozeboom, HJ; Kalk, KH; Huizinga, EG; Dijkstra, BW; Huizinga, Eric G.; Dijkstra, Bauke W.

Published in:
The Journal of Biological Chemistry

DOI:
10.1074/jbc.M109403200

Publication date:
2002

THE JOURNAL OF BIOLOGICAL CHEMISTRY
Vol. 277, No. 5, Issue of February 1, pp. 3727–3732, 2002

Printed in U.S.A.

Crystal Structure of Quinohemoprotein Alcohol Dehydrogenase from *Comamonas testosteroni*

STRUCTURAL BASIS FOR SUBSTRATE OXIDATION AND ELECTRON TRANSFER*

Received for publication, September 28, 2001, and in revised form, November 19, 2001
Published, JBC Papers in Press, November 19, 2001, DOI 10.1074/jbc.M109403200

Arthur Oubrie‡§, Henriëtte J. Rozeboom‡, Kor H. Kalk, Eric G. Huizinga¶, and Bauke W. Dijkstra‖

From the Laboratory of Biophysical Chemistry and BIOSON Research Institute, University of Groningen, Nijenborgh 4, 9747 AG Groningen, The Netherlands

Quinoprotein alcohol dehydrogenases are redox enzymes that participate in distinctive catabolic pathways that enable bacteria to grow on various alcohols as the sole source of carbon and energy. The x-ray structure of the quinohemoprotein alcohol dehydrogenase from *Comamonas testosteroni* has been determined at 1.44 Å resolution. It comprises two domains. The N-terminal domain has a β-propeller fold and binds one pyrroloquinoline quinone cofactor and one calcium ion in the active site. A tetrahydrofuran-2-carboxylic acid molecule is present in the substrate-binding cleft. The position of this oxidation product provides valuable information on the amino acid residues involved in the reaction mechanism and their function. The C-terminal domain is an α-helical type I cytochrome *c* with His^{608} and Met^{647} as heme-iron ligands. This is the first reported structure of an electron transfer system between a quinoprotein alcohol dehydrogenase and cytochrome *c*. The shortest distance between pyrroloquinoline quinone and heme *c* is 12.9 Å, one of the longest physiological edge-to-edge distances yet determined between two redox centers. A highly unusual disulfide bond between two adjacent cysteines bridges the redox centers. It appears essential for electron transfer. A water channel delineates a possible pathway for proton transfer from the active site to the solvent.

Bacteria have versatile metabolic pathways that enable them to adapt to different environmental conditions. Many Gram-negative bacteria, for example, can grow on compounds as different as methylamine, ethanol, and glucose as their sole source of carbon and energy (1–3). The crucial, first step in the catabolism of such compounds is often an oxidation reaction catalyzed by a class of periplasmic enzymes called quinoproteins. Quinoproteins are oxidoreductases that possess one of four different quinone compounds instead of nicotinamide or flavin cofactors (4–7). They oxidize a wide variety of alcohol- and amine-containing substrates to the corresponding aldehydes or ketones. Proteins containing the pyrroloquinoline quinone (PQQ)[1] cofactor form the best characterized and largest quinoprotein subclass (8). Two different types of PQQ-containing alcohol dehydrogenases (ADHs) have been characterized. The first type includes quinoprotein ethanol dehydrogenases (EDHs) from several *Pseudomonas* species (9–11) and quinoprotein methanol dehydrogenases (MDHs) from methylotrophic bacteria (12). The second type of PQQ-dependent ADHs is the quinohemoprotein alcohol dehydrogenases (QH-ADHs). In addition to PQQ, these latter enzymes contain a covalently bound heme *c*. Both soluble monomeric QH-ADHs (2, 11, 13–16) and membrane-associated enzymes that consist of several subunits (17–19) have been described.

No three-dimensional structures of QH-ADHs are known. In contrast, several x-ray structures have been reported of type I quinoprotein ADHs (20–24) and a soluble quinoprotein glucose dehydrogenase (sGDH) (25). sGDH-inhibitor (26) and sGDH-substrate (27) complexes have provided detailed insights into the dehydrogenation reaction. A recent MDH structure revealed the presence of a PQQ intermediate in the catalytic mechanism (28). These data have clearly shown how sGDH and MDH react with their substrates and, although no information has so far been available to substantiate this hypothesis, it has been argued that the same mechanism operates in the other quinoprotein ADHs (29). In contrast, much less is known about how these enzymes catalyze the electron transfer reactions from reduced PQQ ($PQQH_2$) to the natural electron acceptors.

To obtain more information about these reactions, the QH-ADH from *Comamonas testosteroni* has been studied extensively (30–33). This enzyme consists of two distinct functional domains. The N-terminal domain binds PQQ and calcium in the active site and is homologous to the PQQ-binding domains of all quinoprotein ADHs. The C-terminal domain has a covalently attached heme *c* and is similar to some cytochrome *c* proteins (33). QH-ADH oxidizes primary alcohols and aldehydes in the PQQ-binding domain (31). Subsequently, protons and electrons are removed from $PQQH_2$. The protons are released into the periplasm, thus contributing to the protonmotive force. The electrons are transferred one by one to the

* This work was supported by the Netherlands Foundation for Chemical Research (CW) with financial aid from the Netherlands Organization for Scientific Research (NWO). The costs of publication of this article were defrayed in part by the payment of page charges. This article must therefore be hereby marked "*advertisement*" in accordance with 18 U.S.C. Section 1734 solely to indicate this fact.

The atomic coordinates and structure factors (code 1KB0) have been deposited in the Protein Data Bank, Research Collaboratory for Structural Bioinformatics, Rutgers University, New Brunswick, NJ (http://www.rcsb.org/).

‡ These authors contributed equally to this work.

§ Recipient of EMBO Long Term Fellowship ALTF57-2000. Present address: European Molecular Biology Laboratory, Structural and Computational Biology Program, Meyerhofstrasse 1, D-69117, Heidelberg, Germany.

¶ Present address: Dept. of Crystal and Structural Chemistry, Bijvoet Center for Biomolecular Research, Utrecht University, Padualaan 8, 3584 CH Utrecht, The Netherlands.

‖ To whom correspondence should be addressed. Tel.: 31-50-3634381; Fax: 31-50-3634800; E-mail: bauke@chem.rug.nl.

[1] The abbreviations used are: PQQ, pyrroloquinoline quinone; ADH, alcohol dehydrogenase; EDH, ethanol dehydrogenase; MDH, methanol dehydrogenase; $PQQH_2$, pyrroloquinoline quinol; QH-ADH, quinohemoprotein alcohol dehydrogenase; sGDH, soluble glucose dehydrogenase; THFA, tetrahydrofurfuryl alcohol; MAD, multiple-wavelength anomalous diffraction; EPR, electron paramagnetic resonance.

TABLE I
Data collection and refinement statistics

Data collection				
Data set	Native	Fe-Pb λ_1	Fe-Pb λ_2	Fe-Pb λ_3
Wavelength (Å)	0.9076	1.74026	0.95000	0.94500
Resolution (Å)	1.44	3.0	2.4	2.4
Completeness (%)[a]	96.2 (87.7)	99.7 (98.8)	95.8 (47.8)	98.2 (67.7)
Redundancy	2.2	1.9	1.8	1.9
R_{sym} (I) (%)[a,b]	5.7 (34.0)	4.6 (11.1)	3.5 (13.0)	5.1 (26.9)
Data with $I > 3\sigma(I)$ (%)[a]	71.2 (33.6)	92.0 (73.9)	82.8 (77.6)	81.3 (51.2)
Refinement		Model		
Resolution limits (Å)	50–1.44	Number of Atoms		6297
R_{cryst} (%)[c]	16.0	Protein + cofactors		5242
R_{free} (%)[c]	18.8	Solvent		1055
Number of reflections	111,086	RMS deviations		
Working set	105,415	from ideal geometry		
Test set	5671	Lengths (Å)		0.005
		Angles (°)		2.0

[a] Highest resolution shell in parentheses.
[b] R_{sym} (I) = $100 \times \Sigma_{hkl}\Sigma_i|I_i(hkl) - \langle I(hkl)\rangle|/\Sigma_{hkl}\Sigma_i I_i(hkl)$.
[c] R-factor = $100 \times \Sigma_{hkl}|F_{obs} - F_{calc}|/\Sigma_{hkl} F_{obs}$ where R_{free} is calculated for a randomly chosen 5% of the reflections omitted from refinement, and R_{cryst} is calculated for the remaining 95% of the reflections included in the refinement.

heme *c* in the C-terminal domain (30, 32); from there they are carried by the blue copper protein azurin to a terminal cytochrome oxidase (34). Alcohol oxidation is thus efficiently coupled to the generation of an electrochemical gradient, which in turn drives ATP synthesis. Further advances in understanding the mechanisms of proton and electron transfer in QH-ADH, and in PQQ-dependent proteins in general, have awaited the determination of the three-dimensional structure of QH-ADH.

EXPERIMENTAL PROCEDURES

Purification and Crystallization—QH-ADH was purified from *C. testosteroni* cells grown on ethanol (31). The enzyme was crystallized using polyethylene glycol 6000 as the precipitant (35). A complete data set was collected to 1.44 Å resolution at beam line X11 at the EMBL outstation in Hamburg, Germany and then processed and reduced with the DENZO/SCALEPACK package (36) (Table I).

Structure Determination—The orientation and position of the PQQ domain were determined by molecular replacement using the program EPMR (37) with the PQQ-dependent EDH from *Pseudomonas aeruginosa* (38% sequence identity to QH-ADH in 567 amino acids, Rutgers Protein Data Bank accession code 1FLG, Ref. 24) as the search model. The six best solutions were very similar, having a correlation coefficient of 26.7% and an *R*-factor of 54.7%. The model was improved by rigid body refinement and several cycles of manual rebuilding using the program O (39) and refinement using the simulated annealing protocol from CNS (40). For refinement, 5% of all reflections were set aside for the calculation of R_{free} (41).

At this point it was impossible to recognize features in the electron density that could account for the presence of the heme *c* domain. Moreover, exhaustive rotational searches using numerous cytochrome *c* models were unsuccessful. Therefore, alternative methods were used to determine the structure of the cytochrome domain. First, a multiple-wavelength anomalous diffraction (MAD) data set was collected at beam line BM14 at the ESRF in Grenoble, France (Table I). These data were processed and reduced with DENZO/SCALEPACK (36). Although the MAD data did not yield good phases, anomalous and dispersive Patterson maps calculated with programs from the CCP4 suite (42) showed intense peaks and clearly identified the position of iron, and thereby that of heme *c*, in the unit cell. Secondly, QH-ADH crystals have special optical properties. When viewed under plane-polarized light, their intense orange color caused by the presence of the heme group disappears completely. This property was used to show that the heme rings in the crystals are oriented within 10° of the *c* axis and parallel to the crystallographic *b* axis (35). With this information, a heme group could be positioned correctly in the electron density.

Refinement—After many rounds of alternated model building and refinement using various protocols from CNS (40), the electron density maps improved considerably and the auto-building routine of the ARP-WARP package (43) was used to trace the model. Further refinement resulted in a final model consisting of one QH-ADH monomer (residues 1–675), one calcium ion, one PQQ and one heme *c* cofactor, 1029 water molecules, and three glycerol molecules. Three residues (Asn^{181}, Gly^{182}, and Gly^{566}) are different from the published amino acid sequence (33), and Trp^{512} has been modified to contain a hydroxyl group attached to its CD1 atom. A large fragment of electron density, present in the active site, has been modeled as tetrahydrofuran-2-carboxylic acid.

Coordinates—Coordinates and structure factors have been deposited with the Research Collaboratory for Structural Bioinformatics Protein Data Bank (38) (PDB accession code 1KB0).

RESULTS AND DISCUSSION

Overall Structure—The three-dimensional structure of QH-ADH (677 residues) consists of two distinct domains connected by a long linker (residues 567–590), which spans the whole length of the protein (Fig. 1). The respective orientation of the two domains is completely different from that published in a rudimentary homology model (44). The cytochrome domain is located on top of the dehydrogenase. The edge-to-edge distance and the angle between PQQ and heme *c* are 12.9 Å and 74°, respectively. The surface area buried between the two domains, as calculated with the program Surface (42), is 1028 $Å^2$ on each domain. Direct interdomain contacts (ignoring the connecting loop) involve residues 66–67, 109–110, 113, 118, 430–437, 440, 446, 541, and 546–550 from the dehydrogenase and residues 598, 601–607, 609, 614–619, 643–646, 648, and 653 from cytochrome *c*. Most of these interactions are hydrophobic. In addition, 16 direct and several solvent-mediated hydrogen bonds stabilize the respective orientation of the domains. Two different channels can be identified in the structure: one leads from the solvent to the PQQ-binding site, whereas the other contains a chain of hydrogen-bonded water molecules that connects the bulk solvent to a cavity between the two domains.

The PQQ-binding Alcohol Dehydrogenase Domain—The N-terminal domain (residues 1–566) has a β-propeller fold (Fig. 1) and is very similar to the PQQ-binding domains of MDH (21–23) and EDH (24). The core of the structure is formed by eight four-stranded β-sheets arranged in a radial manner. Six of the eight β-sheets contain one copy of a conserved sequence called the tryptophan-docking motif. The conserved residues cause a tryptophan residue to be buried in a hydrophobic pocket and to stack onto the peptide bond of a glycine residue located on a neighboring β-sheet. The tryptophan-docking motif probably stabilizes the β-propeller fold. It has been described in more detail for MDH (22, 23) and EDH (24).

PQQ is located near the top of the β-propeller in a hydrophobic cavity that is accessible through a deep and narrow channel. Because PQQ and its orthoquinone moiety in particular are essentially planar, the cofactor is presumably in the aromatic $PQQH_2$ form. $PQQH_2$ was also shown to be planar in a sGDH-$PQQH_2$-glucose complex (27), whereas oxidized PQQ had a tilted geometry in a high-resolution structure of sGDH

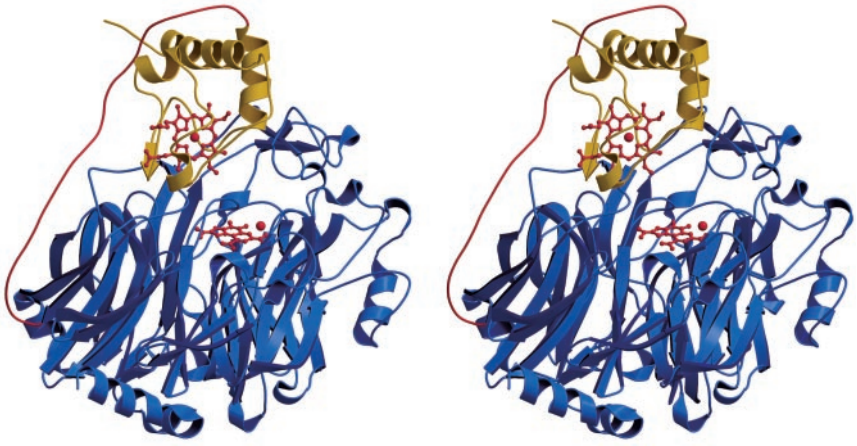

FIG. 1. **Side-by-side stereo view of the structure of QH-ADH.** The PQQ-binding domain, the cytochrome *c* domain, and the connecting linker are shown in *blue*, *yellow*, and *red*, respectively. PQQ and heme *c* are shown as *ball-and-stick* models. Residues 574–578, which are part of the linker, have been included in this figure for clarity although there is no convincing electron density for them. These residues are flexible because gel electrophoresis has shown the protein to be intact (not shown). They have not been included in the final model. Figs. 1–3 and 5 were created with Bobscript (57) and rendered with Raster3D (58).

(26). $PQQH_2$ has in-plane hydrogen-bonding interactions with the side chains of Glu^{70}, Arg^{122}, Thr^{167}, Asn^{263}, Asp^{308}, Lys^{335}, Asn^{394}, and Trp^{395}, and the carbonyl oxygen atoms of Ala^{183}, Ala^{184}, and Val^{544} (Fig. 2*A*). In addition, it ligates the active site calcium with its O5, N6, and O7A atoms in an identical fashion to all other PQQ-dependent proteins of known structure. One side of the tricyclic ring system of PQQ stacks on the side chain of Trp^{245}, and the other side interacts with a disulfide bond. This bond is made between the strictly conserved, adjacent cysteines 116 and 117 (Fig. 2*A*). The formation of this vicinal disulfide bond creates an eight-membered ring structure and forces the peptide bond in a nonplanar *trans* configuration. A disulfide bridge between adjacent residues is extremely rare, which suggests that it has an important biological function.

The Cytochrome c Domain—The C-terminal domain (residues 591–677) classifies as a type I cytochrome *c*. The structure is comprised of five α-helical segments that enclose the *c*-type heme (Fig. 1), which is covalently attached to Cys^{604} and Cys^{607} (Fig. 2*B*). The heme-iron is coordinated by His^{608} and Met^{647}, and it is in a low-spin hexa-coordinated state, as was shown previously by electron paramagnetic resonance (EPR) and resonance Raman spectroscopy (31, 32). Two of the methyl groups (CMA and CMB) of the heme are surrounded by hydrophobic residues (Cys^{604}, Leu^{622}, Met^{625}, Ile^{630}, Leu^{633}, Tyr^{629}, Phe^{636}, Val^{637}, Leu^{662}, and Ile^{666}; Fig. 2*B*), as was suggested by nuclear magnetic resonance spectroscopy (32). The other two methyl groups (CMC and CMD) are in a more hydrophilic environment (not shown). The pyrrole ring to which either CMC or CMD is attached experiences an increase in spin density upon addition of PQQ to PQQ-deficient protein. This could be caused by a rotation of the axial heme-iron ligand Met^{647} around its Cγ-Sδ bond (32), but unfortunately the three-dimensional structure does not provide clues about this.

The Substrate-binding Site—The substrate-binding site is located near PQQ in a hydrophobic cavity. This cavity is much larger than that of MDH and EDH and accounts for the relatively broad substrate specificity of QH-ADH. It contains a ring-shaped electron density, which has been interpreted as tetrahydrofuran-2-carboxylic acid (Fig. 3). The presence of this compound in the active site may result from the oxidation of tetrahydrofurfuryl alcohol (THFA) by QH-ADH. The conversions of THFA to tetrahydrofuran-2-carboxylic acid by the 61% identical, THFA-oxidizing QH-ADH from *Ralstonia eutropha* (16, 45) and of bulky primary alcohols to the corresponding acids by the *Comamonas* enzyme (31) have been described. Except for Tyr^{390}, which is replaced by a Phe, all residues that interact with tetrahydrofuran-2-carboxylic acid are identical between the *R. eutropha* and *C. testosteroni*

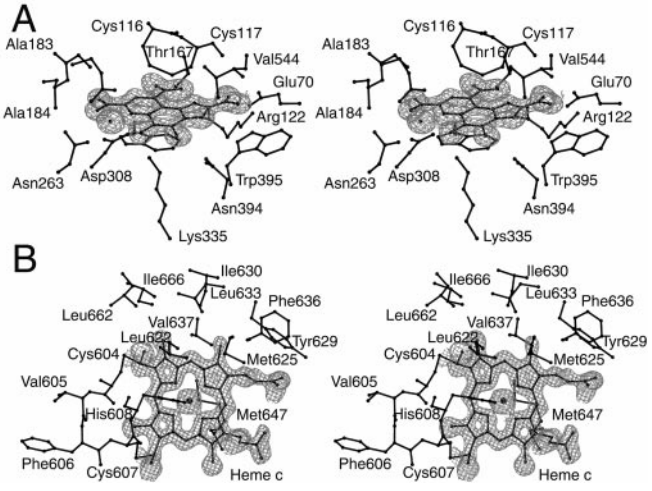

FIG. 2. **Cofactor binding to QH-ADH.** *A*, stereo view of the binding of PQQ and calcium. *B*, stereo view of heme binding. The final σ_A-weighted $2F_o - F_c$ electron density map is shown for both cofactors.

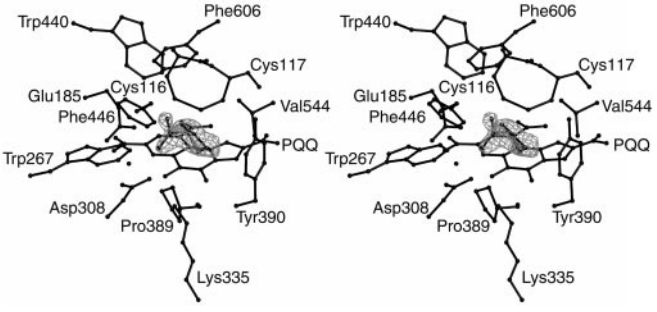

FIG. 3. **Binding of tetrahydrofuran-2-carboxylic acid in the substrate-binding site of QH-ADH.** The final σ_A-weighted $2F_o - F_c$ electron density map is shown for tetrahydrofuran-2-carboxylic acid.

QH-ADHs, making it likely that the *C. testosteroni* enzyme can also degrade THFA. THFA is frequently used as an organic solvent in industry, and therefore it may have contaminated solutions for protein production, purification, and/or crystallization. Tetrahydrofuran-2-carboxylic acid is tightly bound: the tetrahydrofuran ring makes van der Waals contacts with the hydrophobic wall of the cavity formed by residues Trp^{267}, Pro^{389}, Tyr^{390}, Trp^{440}, Phe^{446}, Val^{544}, and Phe^{606} (Fig. 3). The carboxylic acid O2A atom is hydrogen-bonded to Asp^{308} (OD2 atom at 2.3 Å) and Glu^{185} (OE1 at 3.0 Å), whereas the O2B atom is bound to Glu^{185} (OE1 at 2.5 Å), Cys^{116} (SG at 3.0 Å), and Cys^{117} (SG at 2.9 Å). Because these interactions include direct contacts between several carbox-

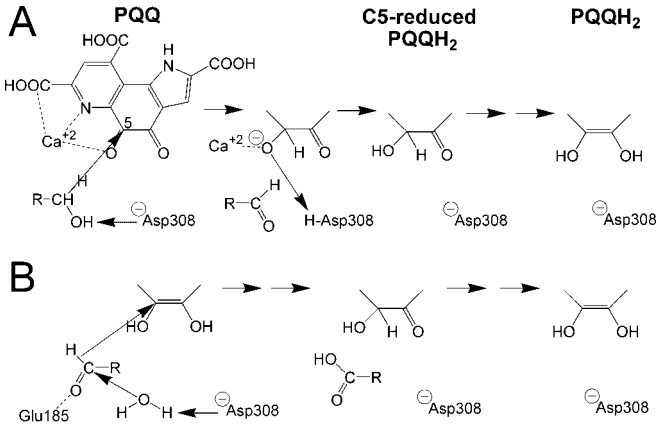

FIG. 4. **Proposed reaction mechanisms for substrate conversion by QH-ADH.** *A*, alcohol oxidation. The reactive C5 atom of PQQ is indicated by the number 5. *B*, aldehyde oxidation.

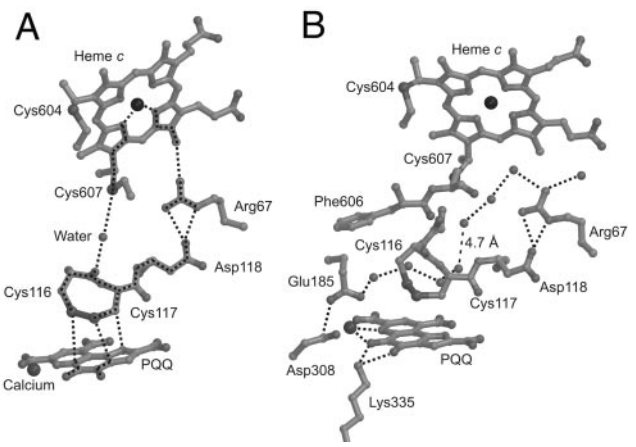

FIG. 5. **Proposed pathways for electron and proton transfer.** *A*, electron transfer. Optimal pathways and one longer alternative are indicated. *B*, proton transfer. Hydrogen bonds are visualized by *black dotted lines*. The gap in the hydrogen-bonding pattern is indicated. Residues possibly involved in either pathway are shown as *ball-and-stick* models.

ylate groups, at least one of them should be in the carboxylic acid form. Unfortunately, this is not resolved in the present x-ray structure. As the product of two subsequent oxidation reactions catalyzed by QH-ADH, tetrahydrofuran-2-carboxylic acid is the first catalytically relevant molecule to be bound in the active site of a Q-ADH. It therefore provides valuable information about the amino acid residues involved in the oxidation reactions of this class of enzymes and their catalytic function, as will be discussed in the next section.

Alcohol and Aldehyde Oxidation—The mechanism of alcohol oxidation has been extensively studied for MDH and sGDH (glucose is a secondary alcohol). These enzymes oxidize their substrates according to a mechanism involving base-catalyzed proton abstraction in concert with direct hydride transfer from the substrate to the C5 atom of PQQ and subsequent tautomerization of the PQQ intermediate to $PQQH_2$ (Fig. 4*A*). The C5 atom is susceptible to nucleophilic addition because of polarization of the C5–O5 bond by calcium (27–29, 46). Because the catalytic machinery of MDH is strictly conserved in QH-ADH, the mechanisms of alcohol oxidation are most likely identical for both enzymes. In QH-ADH, the side chains of Glu^{185} and Asp^{308} ligate the oxygen atoms of tetrahydrofuran-2-carboxylic acid (Fig. 3). Because both amino acid residues are conserved, either one of them could, in principle, act as the general base to catalyze proton abstraction. However, the hydrogen bond between tetrahydrofuran-2-carboxylic acid and Asp^{308} is shorter (2.3 Å) than that between the acid and Glu^{185} (3.0 Å), and in MDH the equivalent of Asp^{308}, not of Glu185, is hydrogen-bonded to the only active site water molecule (28). Moreover, Asp^{308} is in a similar position to His^{144}, the catalytic base in the sGDH (27). These observations suggest the conserved Asp^{308} functions as the catalytic base in the oxidation reactions.

The mechanism of aldehyde oxidation is different from alcohol oxidation because the conversion of an aldehyde into an acid requires the addition of a hydroxyl group. Under the assumption that the same catalytic machinery is used for such a reaction, the following mechanism for the oxidation of aldehydes by QH-ADH may be proposed on the basis of the binding of tetrahydrofuran-2-carboxylic acid in the active site (Fig. 4*B*): Asp^{308} is hydrogen-bonded to a water molecule and the aldehyde substrate is bound with its oxygen atom to the OE1 atom of Glu^{185} and the SG atoms of Cys^{116} and Cys^{117}. Asp^{308} abstracts a proton from the hydrogen-bonded water, and the resultant hydroxyl ion performs a nucleophilic attack on the aldehyde C1 atom to yield the corresponding acid. This occurs in concert with hydride transfer from the aldehyde C1 to the PQQ C5 atom. This mechanism involves a shift in binding position for aldehydes (oxygen atom is bound to Glu^{185}), compared with alcohols (oxygen atom close to Asp^{308}). Kinetic evidence is available to substantiate the existence of such an alternative binding site (30).

Electron Transfer from $PQQH_2$ to Heme c—Because heme *c* is a one-electron acceptor, the two electrons from $PQQH_2$ must be transferred in two separate steps. The PQQ intermediate between these steps is the free-radical PQQH, which was identified by EPR spectroscopy (31). The redox centers and the intervening protein medium in QH-ADH are shown in Fig. 5. The shortest distance between PQQ and heme *c* is 12.9 Å. The conserved disulfide bond between Cys^{116} and Cys^{117} is positioned right between PQQ and heme *c*. Asp^{118} and Arg^{67} are also located between the cofactors. Asp^{118} is conserved in all PQQ-dependent ADHs, including MDHs, whereas Arg^{67} is present in all ADHs with the exception of some MDHs (not shown). Other residues located in the vicinity of the redox sites but not involved in cofactor binding are much less conserved. In addition, several water molecules are located in the interface between the redox centers.

The electron transfer rate in biological systems is strongly related to the edge-to-edge distance between the redox centers involved (47). Electrons can travel up to about 14 Å between two redox centers through the protein medium, but transfer over longer distances always involves additional redox sites (48). The 12.9 Å distance between PQQ and heme *c* is thus one of the longest between functional redox centers determined so far and close to the maximum travel distance of electrons. Using this distance and a calculated value of 0.63 for the atomic density between the two cofactors, a maximum electron transfer rate of $1.0 \times 10^5\ s^{-1}$ could be predicted (48) with the program Harlem (49). This value is much higher than that of substrate oxidation ($k_{cat} = 17\ s^{-1}$), consistent with kinetic data showing that the influence of electron transfer on the kinetic mechanism of QH-ADH is negligible (30).

The intervening protein medium is another important parameter for electron transfer. For PQQ-dependent ADHs, this is stressed by the fact that reduction of the disulfide bond between the active site cysteines in MDH completely abolished electron transfer from MDH to cytochrome c_L (21). The intervening medium may have several different functions in QH-ADH. Given the large separation between PQQ and heme *c*, close to the maximum distance electrons may travel, one function of the medium may be to reduce that distance by providing an additional redox center. In principle, the disulfide bond

between cysteines 116 and 117 could act as such by accepting two electrons and two protons. A disulfide bond involved in redox reactions is indeed located close to an iron-sulfur cofactor in the ferredoxin:thioredoxin reductase system (50). However, biochemical experiments indicate that the disulfide bond of quinoprotein MDH is not reduced during the redox cycle (51), indicating that it does not function as a redox center in PQQ-dependent enzymes.

Alternatively, the active site disulfide bridge may ensure conformational rigidity of the loop between PQQ and heme *c*. This rigidity may be required to maintain the level of nuclear density, which is 0.63 and below the average value of 0.76 (48). Substitution of (one of) the cysteines by other amino acids would thus lead to increased flexibility and possibly to a significantly lower nuclear density, which in turn would have a negative effect on the electron transfer rates.

As a third function, the protein medium could be directly involved in the conduction of electrons. In this case, electron transfer would proceed through specific pathway tubes that may or may not be dynamically controlled (52). The pathways involve covalent bonds, hydrogen bonds, and through-space jumps (53). Optimal electron transfer pathways calculated with Harlem (49) involve atoms of $PQQH_2$, Cys^{116}, Cys^{117}, a water molecule, Cys^{607}, and heme *c* (Fig. 5*A*). A second, longer and therefore possibly less efficient, pathway could include $PQQH_2$, Cys^{117}, Asp^{118}, Arg^{67}, and heme *c*. In conclusion, it appears that the disulfide bond between Cys^{116} and Cys^{117}, and possibly the side chains of Asp^{118} and Arg^{67}, are essential for efficient electron transfer from $PQQH_2$ to heme *c*, whatever their precise function may be.

Proton Transfer from $PQQH_2$ to the Periplasm—Proton pathways usually consist of hydrogen-bonded networks of proton donor and acceptor groups, either water molecules or amino acid side chains (54, 55). Such a network extends from the hydroxyl groups of $PQQH_2$ to the solvent via Lys^{335}, Asp^{308}, Glu^{185}, a water-filled chamber between the two domains, and Arg^{67} (Fig. 5*B*). It is disrupted only once by a distance of 4.7 Å between two water molecules. We propose this network as a channel for proton transfer to the solvent, *i.e.* the periplasm.

Relevance for Other PQQ-dependent Alcohol Dehydrogenases—The physiological electron acceptors of PQQ-dependent ADHs are cytochrome *c* proteins. The redox centers involved in the electron transfer reactions are thus the same. All quinoprotein ADHs including MDH are homologous to QH-ADH, and especially the bridging protein material between the two redox centers is highly conserved. Moreover, the distance between the two cofactors in the complex of MDH and cytochrome c_L was estimated to be 15 Å (56), close to the value observed in QH-ADH. Also, the residues proposed to be involved in proton transfer are conserved. Therefore, the mechanisms of electron and proton transfer may well be identical in all PQQ-dependent ADHs.

In conclusion, the structure of QH-ADH is the first of the type II quinoprotein ADHs. It reveals the presence of tetrahydrofuran-2-carboxylic acid in the active site, and the position of this oxidation product provides valuable information on the amino acid residues involved in the reaction mechanism. Furthermore, the structure shows that electron transfer from $PQQH_2$ to heme *c* is a long-range reaction, for which the presence of a disulfide bond between two adjacent cysteines appears essential. A water channel delineates a possible pathway for proton transfer from $PQQH_2$ to the solvent.

Acknowledgments—We thank the staff of the EMBL outstation at DESY, Hamburg, and of beam line BM 14 at the European Synchrotron Radiation Facility (ESRF), Grenoble, for assistance, the ESRF for support of the work there, and the European Union for support of the work at the EMBL outstation through the HCMP Access to Large Installations Project, Contract Number CHGE-CT-93-0049. We thank Dieter Jendrossek for the strain of *C. testosteroni* and Arjan Snijder and Simon de Vries for stimulating discussions.

REFERENCES

1. Matsumoto, T. (1978) *Biochim. Biophys. Acta* **522,** 291–302
2. Groen, B. W., van Kleef, M. A., and Duine, J. A. (1986) *Biochem. J.* **234,** 611–615
3. van Schie, B. J., Rouwenhorst, R. J., van Dijken, J. P., and Kuenen, J. G. (1989) *Antonie Leeuwenhoek* **55,** 39–52
4. Salisbury, S. A., Forrest, H. S., Cruse, W. B. T., and Kennard, O. (1979) *Nature* **280,** 843–844
5. Janes, S. M., Mu, D., Wemmer, D., Smith, A. J., Kaur, S., Maltby, D., Burlingame, A. L., and Klinman, J. P. (1990) *Science* **248,** 981–987
6. McIntire, W. S., Wemmer, D. E., Chistoserdov, A., and Lidstrom, M. E. (1991) *Science* **252,** 817–824
7. Wang, S. X., Mure, M., Medzihradsky, K. F., Burlingame, A. L., Brown, D. E., Dooley, D. M., Smith, A. J., Kagan, H. M., and Klinman, J. P. (1996) *Science* **273,** 1078–1084
8. Duine, J. A. (1991) *Eur. J. Biochem.* **200,** 271–284
9. Groen, B., Frank, J., Jr., and Duine, J. A. (1984) *Biochem. J.* **223,** 921–924
10. Görisch, H., and Rupp, M. (1989) *Antonie Leeuwenhoek* **56,** 35–45
11. Toyama, H., Fujii, A., Matsushita, K., Shinagawa, E., Ameyama, M., and Adachi, O. (1995) *J. Bacteriol.* **177,** 2442–2450
12. Anthony, C. (2000) *Subcell. Biochem.* **35,** 73–117
13. Yasuda, M., Cherepanov, A., and Duine, J. A. (1996) *FEMS Microb. Lett.* **138,** 23–28
14. Shimao, M., Tamogami, T., Nishi, K., and Harayama, S. (1996) *Biosci. Biotechnol. Biochem.* **60,** 1056–1062
15. Vangnai, A. S., and Arp, D. J. (2001) *Microbiology* **147,** 745–756
16. Zarnt, G., Schrader, T., and Andreesen, J. R. (1997) *Appl. Environ. Microbiol.* **63,** 4891–4898
17. Adachi, O., Tayama, K., Shinagawa, E., Matsushita, K., and Ameyama, M. (1978) *Agric. Biol. Chem.* **42,** 2045–2056
18. Tayama, K., Fukaya, M., Okumura, H., Kawamura, Y., and Beppu, T. (1989) *Appl. Biochem. Biotechnol.* **32,** 181–185
19. Matsushita, K., and Adachi, O. (1993) in *Principles and Applications of Quinoproteins* (Davidson, V. L., ed), pp. 47–63, Marcel Dekker, New York
20. Xia, Z. X., Dai, W. W., Xiong, J. P., Hao, Z. P., Davidson, V. L., White, S., and Mathews, F. S. (1992) *J. Biol. Chem.* **267,** 22289–22297
21. Blake, C. C., Ghosh, M., Harlos, K., Avezoux, A., and Anthony, C. (1994) *Nat. Struct. Biol.* **1,** 102–105
22. Ghosh, M., Anthony, C., Harlos, K., Goodwin, M. G., and Blake, C. (1995) *Structure* **3,** 177–187
23. Xia, Z., Dai, W., Zhang, Y., White, S. A., Boyd, G. D., and Mathews, F. S. (1996) *J. Mol. Biol.* **259,** 480–501
24. Keitel, T., Diehl, A., Knaute, T., Stezowski, J. J., Hohne, W., and Gorisch, H. (2000) *J. Mol. Biol.* **297,** 961–974
25. Oubrie, A., Rozeboom, H. J., Kalk, K. H., Duine, J. A., and Dijkstra, B. W. (1999) *J. Mol. Biol.* **289,** 319–333
26. Oubrie, A., Rozeboom, H. J., and Dijkstra, B. W. (1999) *Proc. Natl. Acad. Sci. U. S. A.* **96,** 11787–11791
27. Oubrie, A., Rozeboom, H. J., Kalk, K. H., Olsthoorn, A. J. J., Duine, J. A., and Dijkstra, B. W. (1999) *EMBO J.* **18,** 5187–5194
28. Zheng, Y. J., Xia, Z., Chen, Z., Mathews, F. S., and Bruice, T. C. (2001) *Proc. Natl. Acad. Sci. U. S. A.* **98,** 432–434
29. Oubrie, A., and Dijkstra, B. W. (2000) *Protein Sci.* **9,** 1265–1273
30. Geerlof, A., Rakels, J. J., Straathof, A. J., Heijnen, J. J., Jongejan, J. A., and Duine, J. A. (1994) *Eur. J. Biochem.* **226,** 537–546
31. de Jong, G. A. H., Geerlof, A., Stoorvogel, J., Jongejan, J. A., de Vries, S., and Duine, J. A. (1995) *Eur. J. Biochem.* **230,** 899–905
32. de Jong, G. A. H., Caldeira, J., Sun, J., Jongejan, J. A., de Vries, S., Loehr, T. M., Moura, I., Moura, J. J., and Duine, J. A. (1995) *Biochemistry* **34,** 9451–9458
33. Stoorvogel, J., Kraayveld, D. E., Van Sluis, C. A., Jongejan, J. A., De Vries, S., and Duine, J. A. (1996) *Eur. J. Biochem.* **235,** 690–698
34. Matsushita, K., Yamashita, T., Aoki, N., Toyama, H., and Adachi, O. (1999) *Biochemistry* **38,** 6111–6118
35. Oubrie, A., Huizinga, E. G., Rozeboom, H. J., Kalk, K. H., De Jong, G. A. H., Duine, J. A., and Dijkstra, B. W. (2001) *Acta Crystallogr. Sect. D Biol. Crystallogr.* **57,** 1732–1734
36. Otwinowski, Z., and Minor, W. (1997) *Methods Enzymol.* **276,** 307–326
37. Kissinger, C. R., Gehlhaar, D. K., and Fogel, D. B. (1999) *Acta Crystallogr. Sect. D Biol. Crystallogr.* **55,** 484–491
38. Berman, H. M., Westbrook, J., Feng, Z., Gilliland, G., Bhat, T. N., Weissig, H., Shindyalov, I. N., and Bourne, P. E. (2000) *Nucleic Acids Res.* **28,** 235–242
39. Jones, T. A., Zou, J.-Y., Cowan, S. W., and Kjeldgaard, M. (1991) *Acta Crystallogr. Sect. A* **47,** 110–119
40. Brunger, A. T., Adams, P. D., Clore, G. M., DeLano, W. L., Gros, P., Grosse-Kunstleve, R. W., Jiang, J. S., Kuszewski, J., Niles, M., Pannu, N. S., Read, R. J., Rice, L. M., Simonson, T., and Warren, G. L. (1998) *Acta Crystallogr. Sect. D Biol. Crystallogr.* **54,** 905–921
41. Brünger, A. T. (1992) *Nature* **355,** 472–475
42. Collaborative Computational Project Number 4. (1994) *Acta Crystallogr. Sect. D Biol. Crystallogr.* **50,** 760–763
43. Perrakis, A., Morris, R., and Lamzin, V. S. (1999) *Nat. Struct. Biol.* **6,** 458–463
44. Jongejan, A., Jongejan, J. A., and Duine, J. A. (1998) *Protein Eng.* **11,** 185–198
45. Zarnt, G., Schrader, T., and Andreesen, J. R. (2001) *J. Bacteriol.* **183,** 1954–1960
46. Dewanti, A. R., and Duine, J. A. (2000) *Biochemistry* **39,** 9384–9392

47. Moser, C. C., Keske, J. M., Warncke, K., Farid, R. S., and Dutton, P. L. (1992) *Nature* **355,** 796–802
48. Page, C. C., Moser, C. C., Chen, X., and Dutton, P. L. (1999) *Nature* **402,** 47–52
49. Kurnikov, I. V. (2000) *Harlem Computer Program*, University of Pittsburgh, Pittsburgh
50. Dai, S., Schwendtmayer, C., Schurmann, P., Ramaswamy, S., and Eklund, H. (2000) *Science* **287,** 655–658
51. Avezoux, A., Goodwin, M. G., and Anthony, C. (1995) *Biochem. J.* **307,** 735–741
52. Balabin, I. A., and Onuchic, J. N. (2000) *Science* **290,** 114–117
53. Beratan, D. N., Onuchic, J. N., Winkler, J. R., and Gray, H. B. (1992) *Science* **258,** 1740–1741
54. Iwata, S., Ostermeier, C., Ludwig, B., and Michel, H. (1995) *Nature* **376,** 660–669
55. Stowell, M. H., McPhillips, T. M., Rees, D. C., Soltis, S. M., Abresch, E., and Feher, G. (1997) *Science* **276,** 812–816
56. Harris, T. K., and Davidson, V. L. (1993) *Biochemistry* **32,** 14145–14150
57. Esnouf, R. M. (1997) *J. Mol. Graph.* **15,** 132–134
58. Merritt, E. A., and Bacon, D. J. (1997) *Methods Enzymol.* **277,** 505–524